31st Annual International Conference of the IEEE EMBS
Minneapolis, Minnesota, USA, September 2-6, 2009

Volume Conductor Effects on Simulated Magnetogastrograms

Wenlian Qiao, Rié Komuro, Andrew J Pullan and Leo K Cheng

Abstract— **We simulated the magnetic field due to gastric electrical activity (GEA) using a temporally and spatially moving dipole source. The contributions of the volume conductor to the total magnetic field were examined. The volume conductor was represented using three simplified models (free-space, spherical and half-space) and an anatomically realistic torso model. We compared the patterns and the directions of the resultant magnetic fields generated using these volume conductor models. We concluded that all the simplified models produced significantly different magnetic fields when compared to the anatomically realistic model. Therefore, an anatomically realistic model is necessary for any modeling studies to accurately calculate the magnetic fields from GEA.**

I. INTRODUCTION

In the gastrointestinal system, there is a periodic electrical activity (termed slow waves) that underlies gut contractions. Slow wave disorders are widely considered to contribute to many clinical dysmotility disorders. Digestive motility diseases are estimated to affect thirty-five million people in the United States [1]. Therefore, the ability to non-invasively characterize gastric slow wave activity would be a highly beneficial diagnostic aid. The electrical events in the smooth muscle of the gastrointestinal tract produce electric fields and magnetic fields [2]. The measurement of the magnetic fields via SQUID (Superconducting QUantum Interference Device) magnetometers has been shown to provide information about the underlying electrical events [3]. In simulations, the electrical activity in the stomach is usually represented by electrical current dipoles [4]. The magnetic field due to a dipole embedded in a conducting medium is composed of two main components. One component is the magnetic field due to the dipole in free space and the second component is due to the effect of the interfaces between regions of different electrical conductivities within the volume conductor [5]. Usually, the volume conductor component is either assumed to be negligible [6] or the volume conductor itself has been assumed to have a simplified geometry [7], [8], [9], [10], [11]. In this paper, we show the simulated magnetic fields due to gastric electrical activity (GEA) and illustrate the effects of the volume conductor geometry upon the resultant magnetic fields. Specifically, we model the volume conductor as a free-space, a sphere, a half-space and an anatomically realistic torso derived from CT images. We aim to determine the accuracy of using the mathematical models of the simplified geometries to calculate the magnetic fields when compared to using the mathematical model of an anatomically realistic torso geometry.

Manuscript received on March 31, 2009. This work was funded in part by a grant from the National Institutes of Health (NIH R01 DK64775) and a University of Auckland International Doctoral Scholarship.

Wenlian Qiao is with the Auckland Bioengineering Institute, the University of Auckland (Private Bag 92019 Auckland 1142, New Zealand; Tel: +64 9 373 7599 x 89742; fax: +64 9 367 7157; email: wqia007@aucklanduni.ac.nz)

Rié Komuro and Leo K Cheng are with the Auckland Bioengineering Institute, the University of Auckland.

Andrew J Pullan is with the Department of Engineering Science, and a principal investigator at the Auckland Bioengineering Institute, the University of Auckland.

II. METHODS AND RESULTS

The magnetic fields external to the body were simulated using a single moving dipole source derived from a slow wave simulation of GEA [12]. The dipole had both a temporally moving centre and orientation and represented a single normal slow wave propagating down the length of the stomach. The associated magnetic fields were calculated using the mathematical models representing different volume conductor geometries illustrated schematically in Fig. 1. Analytic functions were used to calculate the magnetic fields for the free-space, sphere and half-space models and numerical integration was used for the anatomically realistic torso model. The magnetic fields used to compare the different models were calculated at 19 field positions corresponding to the channels of the SQUID that had been optimized for measuring the magnetic fields resulting from GEA [13].

A. Calculation of Magnetic Fields

The magnetic field due to a dipole source embedded in a conducting medium is comprised of two major components - the "primary source" due to the electric current dipole itself and the "secondary source" due to the volume conductor. These components are denoted as $\mathbf{B_d}$ and $\mathbf{B_v}$ respectively in Eqn. 1 computing the magnetic field $\mathbf{B}$:

$$\mathbf{B} = \mathbf{B_d} + \mathbf{B_v}, \tag{1}$$

The magnetic field due to the single dipole itself can be calculated relatively simply:

$$\mathbf{B_d}(\mathbf{r_f}) = \mu_0 \frac{\boldsymbol{\rho} \times \mathbf{r}}{4\pi r^3}, \tag{2}$$

where $\mathbf{r_f}$ is the field point vector where the magnetic field is calculated, μ_0 is the permeability of the free space, $\boldsymbol{\rho}$ is the dipole moment vector that reflects the strength of a dipole, $\mathbf{r}$ is the displacement vector from a dipole centre to the field point and the corresponding distance is denoted by r. This formula is often referred to as the free-space model [14]. The calculation of the "secondary source" is given by:

$$\mathbf{B_v}(\mathbf{r_f}) = -\frac{\mu_0}{4\pi} \sum_{j=1}^{n} \sigma_j \int_G \bigtriangledown \phi(\mathbf{r_d}) \times \frac{\mathbf{r}}{r^3} d\Omega_j \text{ for } j = 1...n \tag{3}$$

where n is the number of regions within the volume conductor and each of the regions has a different electrical conductivity, σ_j. The surface integral is over the region, G and $\phi(\mathbf{r_d})$ is the electric potential due to the dipole source located at $\mathbf{r_d}$. The calculation of $\mathbf{B_v}$ is more complex especially when the volume conductor has an irregular geometry. For this reason, the volume conductor effects are often ignored [6] or the geometry is simplified to idealized geometries such as spheres, ellipses, and planes [7], [8], [9], [10], [11].

We used the free-space, sphere, half-space and anatomically realistic torso models as illustrated schematically in Fig. 1 to calculate magnetic fields. The simplified volume conductor models calculate the primary and secondary sources of magnetic field implicitly and represent the total magnetic field.

The external magnetic field due to a dipole located inside a sphere volume conductor is given by [14]:

$$\mathbf{B}(\mathbf{r_f}) = \frac{\mu_0}{4\pi M^2}(M\boldsymbol{\rho} \times \mathbf{r_d} - \boldsymbol{\rho} \times \mathbf{r_d} \bullet \mathbf{r_f} \bigtriangledown M), \qquad (4)$$

where

$$M = r(r_f r + {r_f}^2 - \mathbf{r_d} \bullet \mathbf{r_f}),$$

$$\bigtriangledown M = (\frac{r^2}{r_f} + \frac{\mathbf{r} \bullet \mathbf{r_f}}{r} + 2r + 2r_f)\mathbf{r_f} - (r + 2r_f + \frac{\mathbf{r} \bullet \mathbf{r_f}}{r})\mathbf{r_d}.$$

It should be noted that the radius of the sphere is not included as a parameter in this formula, as it has no effect upon the magnetic field. The half-space model has been derived from the sphere model in Eqn. 4, where the limit of the radius of the sphere has been extended to infinity [14]. The full magnetic field on one side of the half plane due to a dipole located on the other side of the plane is given by [14]:

$$\mathbf{B}(\mathbf{r_f}) = \frac{\mu_0}{4\pi K^2}(\boldsymbol{\rho} \times \mathbf{r} \bullet \mathbf{e_z} \bigtriangledown K - K\mathbf{e_z} \times \boldsymbol{\rho}), \qquad (5)$$

where

$$K = r(r + \mathbf{r} \bullet \mathbf{e_z}),$$

$$\bigtriangledown K = (2 + \frac{\mathbf{r} \bullet \mathbf{e_z}}{r})\mathbf{r} + r\mathbf{e_z},$$

and $\mathbf{e_z} = \begin{bmatrix} 0 & 0 & 1 \end{bmatrix}^T$ is a unit vector in the normal direction of the half plane. The anatomically realistic torso was derived from CT images of a male volunteer [12]. The torso model was defined by 254 nodes and 264 elements interpolated using bicubic Hermite basis functions. The primary and secondary sources for this model were calculated explicitly by solving Eqns. 2 and 3. The two magnetic field sources $\mathbf{B_d}$ and $\mathbf{B_v}$ were added to give the overall magnetic field external to the torso.

B. Comparison of Volume Conductor Models

To quantify the effects of volume conductor models upon the magnetic field simulations, the electric current dipoles were simulated to represent one slow wave cycle (20 seconds) [12]. The magnetic fields induced by electric current dipoles were calculated at 19 field points.

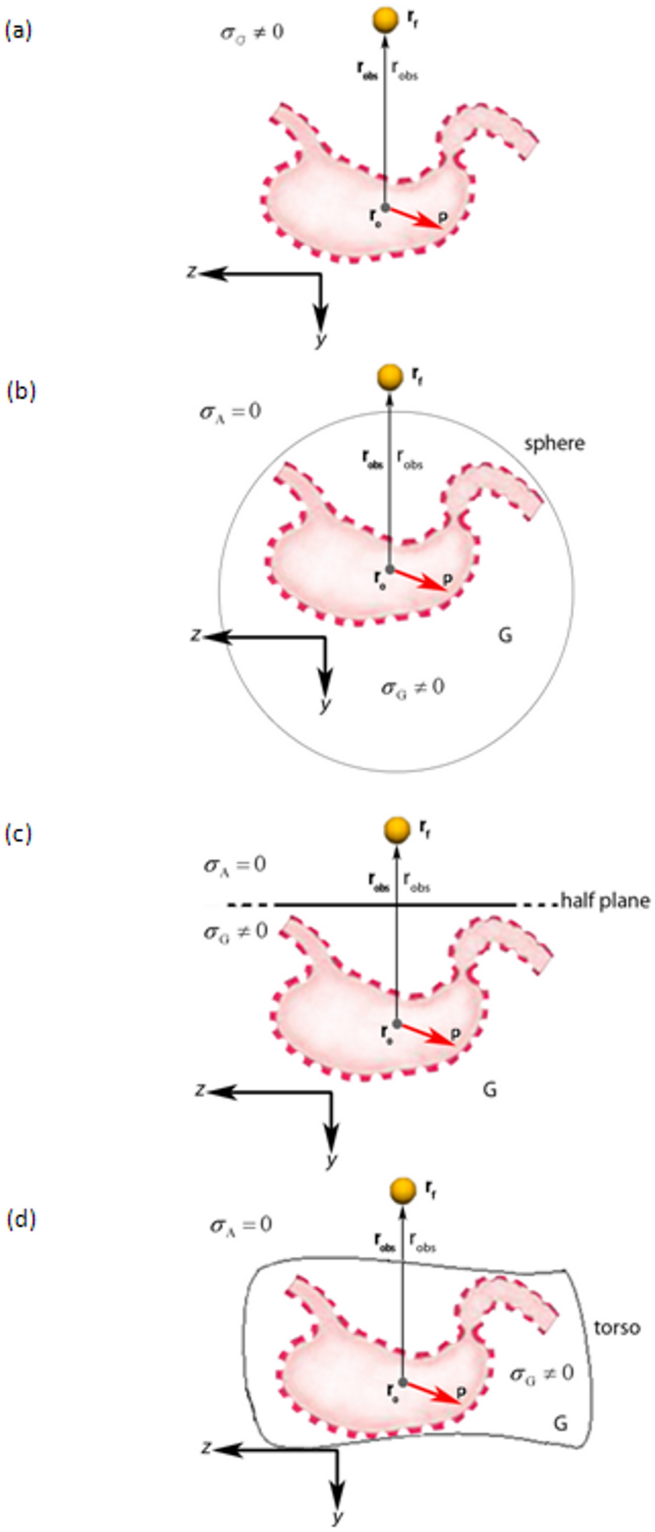

Fig. 1. Schematic diagrams for (a) the free-space model, (b) the sphere model, (c) the halfspace model and (d) the anatomically realistic torso model in the saggital plane. The positive x-direction is into the page. Parameters σ_G and σ_A are the electrical conductivities in the conductive and nonconductive regions, respectively. Vectors $\mathbf{r_o}$, $\mathbf{rf}$ are the coordinates of the dipole centre and field points from the origin, and vector $\mathbf{r_{obs}}$ is the displacement from the dipole centre to the field points. The dotted outline of the stomach was not explicitly included in the volume conductor models and is shown for illustrative purposes.

1) Effects on Magnetic Field Magnitudes/Distribution: To investigate the differences in magnitude between the magnetic fields of the simplified volume conductor models and the anatomically realistic torso model, the magnetic fields at 19 field points were interpolated by using a linear mesh function in MATLAB (http://www.mathworks.com). Fig. 2 shows the magnetic field maps of different volume conductor models at t=10 s, which is in the middle of the simulated slow wave cycle. The free-space model generally resulted in the largest magnetic field, except in the y-direction. The magnetic field distribution of the half-space model was the closest to the distribution of the anatomically realistic torso model.

2) Effects on Magnetic Field Distributions: To investigate the differences in direction between the magnetic fields of the simplified volume conductor models and the anatomically realistic torso model, the angles between the magnetic field vectors of the simplified volume conductor models and the anatomically realistic torso model were calculated at 19 field points and averaged spatially for each time step. The results are summarized in Fig. 3. The magnetic field direction of the half-space model was the closest to the magnetic field direction of the anatomically realistic torso model. However, the differences between the direction of the magnetic field of the half-space model and that of the anatomically realistic torso model could be as large as 80 degrees at specific time instances (e.g. at t=8 s). None of the simplified volume conductor models was able to produce the magnetic field in the same direction as that of the anatomically realistic torso.

3) Effects on Secondary Sources: Previous studies have shown that the geometry of the volume conductor affects the secondary source of magnetic field [5], [15]. To quantify this statement, the secondary sources of the simplified volume conductor models were compared to the secondary sources of the anatomically realistic torso model. Fig. 4 shows the spatially and temporally averaged secondary sources of different volume conductor models. All the volume conductor models had smaller secondary sources in the y-direction when compared to the other principle directions. The half-space model had no secondary source in the y-direction. However, the spatially and temporally averaged magnitude of the secondary source from the anatomically realistic torso model in the y-direction was 0.7 pT. On average, the secondary source of the half-space model was the closest to the secondary source of the anatomically realistic torso model.

III. DISCUSSION AND CONCLUSIONS

A volume conductor can be broadly divided into the electric conductive and non-conductive regions. The magnetic field due to a dipole located in the conductive region diminishes at the interface between the two regions when examining the magnetic field in the non-conductive region [5]. The diminishing of the magnetic field is represented by the secondary source of the magnetic field calculated from the volume conductor models. The resistive effect of

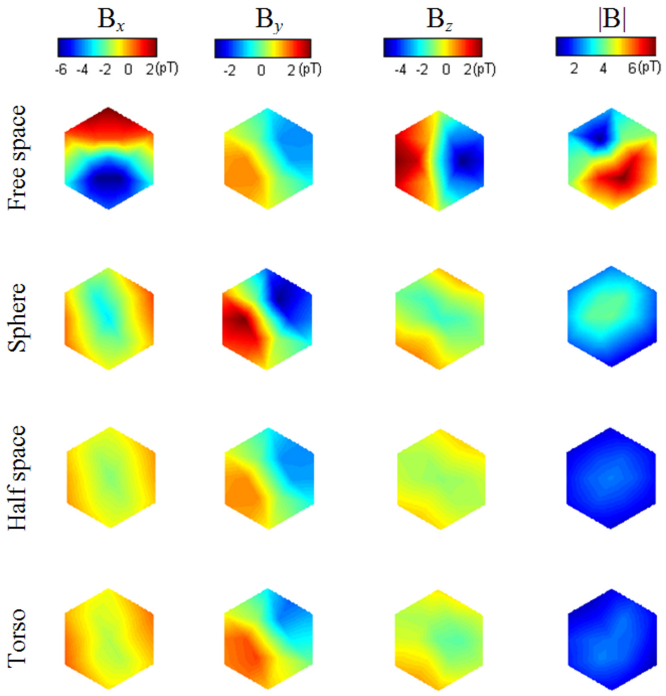

Fig. 2. Magnetic field maps in the x-, y-, z-directions and the magnitudes of magnetic field at t=10 s. The magnetic field maps were produced by interpolating the magnetic field at 19 field points.

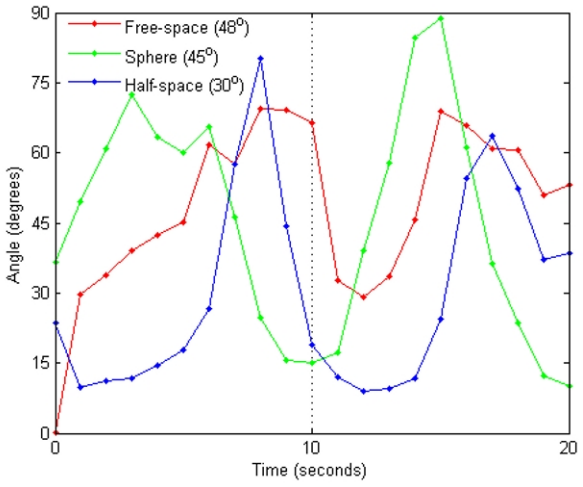

Fig. 3. Spatially average differences in the angle between the magnetic field of the simplified volume conductor models and that of the anatomically realistic torso model. The angles were calculated at 19 field points and averaged spatially at each time instance. The bracketed values are the spatially and temporally averaged angle difference between the corresponding model and the anatomically realistic torso model.

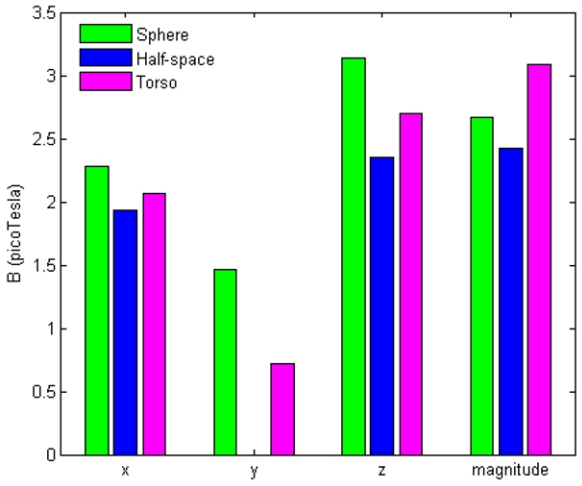

Fig. 4. Comparison between the spatially and temporally averaged secondary magnetic field of the sphere, half-space and anatomically realistic torso models. The secondary sources were calculated by rearranging Eqn. 1.The half-space model had no secondary source in the *y*-direction.

the interface decreases as the size of the volume conductor increases. The free-space model represents an infinitely large volume conductor. Thus the calculated magnetic fields from the free-space model are in larger magnitudes when compared to the magnetic fields from other volume conductor models as shown before. In the half-space model, the position of the half plane approximates the position of the frontal wall of the anatomically realistic torso. Thus the half-space volume conductor has the most similar electric conductive and non-conductive interface geometry as the anatomically realistic torso volume conductor. As expected, the half-space model and the anatomically realistic torso model resulted in the most closely matched magnetic fields. As the secondary sources do not contribute to the magnetic field in the direction perpendicular to the surface of the volume conductor [5], the half-space model did not have a secondary source in the *y*-direction. In contrast, the anatomically realistic torso model had an average secondary source of 0.7 pT in the *y*-direction (Fig. 4), which was a significant proportion of the practically recorded magnetic field of 2-6 pT [3], [13]. We believe that the realistic shape of the volume conductor is important in magnetic field simulations. Accurate torso modeling is crucial in examining magnetic fields in the direction that is not tangential to the body.

It should be noted that the results from idealized volume conductor models were only compared to one torso geometry in our study. The volume conductor was also assumed to be homogenous with the alternating muscle and fat layers ignored. In the future work, more torso models with more realistic anatomy will be investigated.

IV. ACKNOWLEDGMENTS

The authors wish to thank Prof. L. Alan Bradshaw of Vanderbilt University for his input. The authors would also like to thank Profs. John Wikswo, Brad Roth and Geertjan Huiskamp for their assistance with the calculations of the analytic magnetic fields.

REFERENCES

[1] John Hopkins Medicine, *Motility and digestive disorders*. Avaiable: http://www.hopkinsbayview.org.

[2] L.K. Cheng, G. O'Grady, P Du, J.U. Egbuji, J.A. Windsor and A.J. Pullan. Gastrointestinal System. Wiley Interdisp Rev: System Biology and Medicine, 2009. In press.

[3] W.O. Richards, L.A. Bradshaw, D.J. Staton, C.L. Garrard, F. Liu, S. Buchanan and J.P. Wikswo, Jr., "Magnetoenterography (MENG): non-invasive measurement of bioelectric activity in human small intestine," *Dig. Dis.*, vol. 41, pp. 2293-2301, 1996.

[4] L.A. Bradshaw, A. Myers, J.P. Wikswo, W.O. Richards, "A spatio-temporal dipole simulation of gastrointestinal magnetic fields," *IEEE Trans Biomed Eng.*, vol. 50 (7), pp. 836-847, 2003.

[5] R. Plonsey, "The nature of sources of bioelectric and magnetic fields," *Biophys J.*, vol. 39 (3), pp. 309-312, 1982.

[6] D. Rose, E. Ducla-Soares and S. Sato, "Improved accuracy of MEG localization in the temporal region with inclusion of volume current effects," *Brain Topogr.*, vol. 1, pp. 175-181, 1989.

[7] G. Dassios and G. Kariotou, "Magnetoencephalography in ellipsoidal geometry," *J Math Phys*, vol. 44, pp. 220-241, 2003.

[8] T. Miyashita, A. Kandori, K. Tsukada, M. Sato, Y. Terada, M. Sato, Y. Terada, H. Horigome and T. Mitsui, "Construction of tangential vectors from normal cardiac magnetic field components," *Proceedings of 20th Ann. Int. Conference IEEE*, vol. 20, pp. 520-523, 1998.

[9] H. Hallez, B. Canrumste, R. Grech, J. Muscat, W. DeClercq, A. Verqult, Y. D'Asseler, K.P. Camilleri, S.G. Fabri, S. Van Huffel and I. Lemahieu, "Review on solving the forward problem in EEG source analysis," *J Neuroeng Rehabil*, vol. 4, pp. 46, 2007.

[10] L.A. Bradshaw, A. Irimia, J.A. Sim and W.O. Richards, "Biomagnetic signatures of uncoupled gastric musculature," *Neurogastroenterol Motil*, vol. 6, pp. 1189-1203, 2009.

[11] A. Irimia, "Calculation of the magnetic field due to a bioelectric current dipole in an ellipsoid," *App Math*, vol. 53, pp. 131-142, 2008.

[12] R. Komuro, L.K. Cheng and A.J. Pullan, "Comparison and analysis of inter-subject variability of simulated magnetic activity generated from gastric electrical activity," *Ann Biomed Eng.*, vol. 36, pp. 1049-1059, 2008.

[13] L.A. Bradshaw, A. Irimia, J.A. Sims, M.R. Gallucci, R.L. Palmer and W.O. Richards, "Biomagnetic characterization of spatiotemporal parameters of the gastric slow wave," *Neurogastroenterology Motil.*, vol. 18, pp. 619-631, 2006.

[14] J. Sarvas, "Basic mathematical and electromagnetic concepts of the biomagnetic inverse problem," *Phys Med Bio.*, vol. 32, pp 11-12, 1987.

[15] J.C. Mosher, "A review on the importance of volume currents," *14th International Conference on Biomagnetism*, Boston Massachusetts, August 2004.